# Characterizing the Discoloration of Methylene Blue in $Fe^0/H_2O$ Systems.

C. Noubactep

Angewandte Geologie, Universität Göttingen, Goldschmidtstraße 3, D - 37077 Göttingen, Germany.

Tel.: +49 551 39 3191, Fax.: +49 551 399379, e-mail: cnoubac@gwdg.de

## Abstract

Methylene blue (MB) was used as a model molecule to characterize the aqueous reactivity of metallic iron in $Fe^0/H_2O$ systems. Likely discoloration mechanisms under used experimental conditions are: (i) adsorption onto $Fe^0$ and $Fe^0$ corrosion products (CP), (ii) co-precipitation with in-situ generated iron CP, (iii) reduction to colorless leukomethylene blue (LMB). MB mineralization (oxidation to $CO_2$) is not expected. The kinetics of MB discoloration by $Fe^0$, $Fe_2O_3$, $Fe_3O_4$, $MnO_2$, and granular activated carbon were investigated in assay tubes under mechanically non-disturbed conditions. The evolution of MB discoloration was monitored spectrophotometrically. The effect of availability of CP, $Fe^0$ source, shaking rate, initial pH value, and chemical properties of the solution were studied. The results present evidence supporting co-precipitation of MB with in-situ generated iron CP as main discoloration mechanism. Under high shaking intensities (> 150 $min^{-1}$), increased CP generation yields a brownish solution which disturbed MB determination, showing that a too high shear stress induced the suspension of in-situ generated corrosion products. The present study clearly demonstrates that comparing results from various sources is difficult even when the results are achieved under seemingly similar conditions. The appeal for an unified experimental procedure for the investigation of processes in $Fe^0/H_2O$ systems is reiterated.

**Keywords**: Adsorption; Co-precipitation; Iron Corrosion, Methylene Blue; Zerovalent Iron.

## Introduction

Permeable reactive barriers using elemental iron-based alloys ($Fe^0$-based alloys widely termed as zerovalent iron) as a reactive medium have been proven to be an efficient and affordable technology for removing inorganics and organics species from groundwater [1-7]. Even living species like viruses have been successfully removed [8]. Despite 15 years of intensive investigations, the removal mechanisms of contaminants in $Fe^0$ treatment systems are still not well understood [9,10]. In fact, the well-established premise that contaminant removal results from the low electrode potential of the redox couple $Fe^{II}/Fe^0$ ($E^0$ = -0.44 V) can not explain why redox-insensitive species are quantitatively removed [11,12]. However, understanding the nature of primary processes yielding to contaminant removal in $Fe^0/H_2O$ systems is of fundamental importance for advancing technological applications. The accurate knowledge of these processes will favor the identification of factors dominating the general reactivity of $Fe^0/H_2O$ systems, which is of fundamental importance for the long-term stability of iron reactive barriers. A more rational devising of $Fe^0$ treatment systems for an effective and economical contaminant removal could be achieved.

$Fe^0$ oxidation releases dissolved iron species ($Fe^{II}$, $Fe^{III}$) which hydrolyse with increasing pH and precipitate primarily as hydrous oxides (oxide-film) or corrosion products (CP). Oxide-films (CP) of varied composition and thickness develop at all aqueous $Fe^0/H_2O$ interfaces [13,14]. Therefore, an aqueous $Fe^0$ treatment system ($Fe^0/H_2O$ system) is made up of $Fe^0$, iron oxides (oxide-film), and water ($H_2O$). Contaminant adsorption onto the oxide-film and reduction by $Fe^0$ have mostly been evaluated as separate, independent processes that occur simultaneously or sequentially on metal surfaces. However, contaminants may be primarily quantitatively sequestered by in situ generated hydrous iron oxides (co-precipitation) [11,12]. Initial corrosion products polymerise and precipitate, first as very reactive oxides having short-range crystalline

49 order and after aging as crystalline oxides [15-18]. Subsequent abiotic direct reduction (electrons
50 are transferred from $Fe^0$) or indirect reduction (electrons from $Fe^{II}$, $H/H_2$) of adsorbed or co-
51 precipitated contaminants is possible. As a rule co-precipitation occurs whenever the
52 precipitation of a major species (e.g., iron oxide) takes place in the presence of foreign species
53 (e.g., contaminants) and has been documented for organics [16,17,19,20], inorganics [21-23] and
54 living species [8] under various conditions. Generally, adsorption and co-precipitation are
55 considered to be related such that in order for co-precipitation to occur, sorption to the surface of
56 a forming solid occurs and the adsorbed species is then sequestered in the matrix of the
57 precipitating phase (e.g. iron hydroxide). However, co-precipitation in $Fe^0/H_2O$ systems may be
58 primarily regarded as a non-specific removal mechanism [11,17] as to be demonstrated in this
59 study of a process involving the discoloration of methylene blue.
60 Methylene blue (MB) is a well-known redox indicator [24] and is a cationic thiazine dye with the
61 chemical name tetramethylthionine chloride. It has a characteristic deep blue colour in the
62 oxidized state; the reduced form (leukomethylene blue - LMB) is colorless. MB has been widely
63 used in environmental sciences primarily to access the suitability of various materials for
64 wastewater discoloration [25-29]. The mechanism of MB removal by $Fe^0$-based materials which
65 may be suitable for environmental remediation (cast iron, low alloy steel) has not been yet
66 systematically investigated. Imamura et al. [30] investigated the mechanism of adsorption of
67 methylene blue and its congeners onto stainless steel particles. MB has also been used for
68 corrosion inhibition of mild steel in acid solutions [31].
69 The literature on "$Fe^0$ technology" is characterized by the fact that, since the effectiveness of $Fe^0$
70 reactive walls to degrade solvents was demonstrated, the feasibility of applying $Fe^0$ to treat other
71 compounds (or group of compounds) are performed without previous systematic investigations
72 [9]. For example, while presenting the discoloration of MB by a Fe/Cu bimetallic system, Ma et

al. [28] referenced several works dealing with dyes in general [32-34]. The authors did not specified whether the referenced works have used MB. Furthermore, their experimental procedure did not include a system with $Fe^0$ alone to evidence the improvement induced by $Cu^0$ addition.

Given the diversity of contaminant removal mechanisms in a $Fe^0/H_2O$ system, an approach to elucidate the mechanism of contaminant removal in the system is to characterise the removal process of the contaminant in question by a pure adsorbent (e.g. activated carbon - AC), and model iron corrosion products ($Fe_2O_3$, $Fe_3O_4$) under the same experimental conditions [35]. Here, comparing the evolution of contaminant removal in the systems with pure adsorption (AC, $Fe_2O_3$, $Fe_3O_4$) and in the system with $Fe^0$ will help discussing the removal mechanism. Another approach consists in introducing $MnO_2$ to delay the availability of corrosion products in the system [36]. $MnO_2$ readily reacts with $Fe^{II}$ from $Fe^0$ corrosion products: reductive dissolution of $MnO_2$ by $Fe^{II}$ [37]. If the process of contaminant removal is coupled with the precipitation of iron, then contaminant removal will be delayed as long as the added amount of $MnO_2$ consumes $Fe^{II}$ for reductive dissolution as it will be presented later.

The present study is an attempt to elucidate the physico-chemical mechanism of MB discoloration in $Fe^0/H_2O$ systems by comparing the kinetics and/or the extent of MB discoloration by $Fe^0$ and different materials: granular activated carbon (GAC or AC), iron oxides ($Fe_2O_3$, $Fe_3O_4$) and manganese dioxide ($MnO_2$). Non-disturbed (not shaken or shaking at 0 $min^{-1}$) batch experiments were performed in order to allow formation and transformation of corrosion products at the surface of $Fe^0$ as it occurs in the nature and in column experiments. The effects of various factors (initial pH value, mixing intensity, particle size, $Fe^0$ source, $Cl^-$, $HCO_3^-$, EDTA) on the extent of MB discoloration are discussed. The results show that MB quantitative

discoloration is mostly due to co-precipitation with in-situ generated corrosion products. Therefore, MB discoloration occurs within the oxide-film on $Fe^0$.

**Background of the Experimental Methodology**

A survey of the electrode potentials of the redox couples relevant for the discussion in this study [$Fe^{II}_{(aq)}/Fe^0$, $Fe^{III}_{(aq)}/Fe^{II}_{(aq)}$, $Fe^{III}_{(s)}/Fe^{II}_{(s)}$, $MnO_2/Mn^{2+}$, $O_2/HO^-$, and $MB^+$/LMB (Eq. 1 to Eq. 6)] suggests that from the available iron species, $Fe^0$ and $Fe^{II}_{(s)}$ can reduce MB. Equation 2 is that of the adsorbed $Fe^{II}$ known as structural $Fe^{II}$. The electrode potential of this redox couple was determined by White and Patterson [38]. The electrode potential of Eq. 3 to 6 shows that $Fe^{III}_{(aq)}$, dissolved $O_2$ and $MnO_2$ may re-oxidize colorless LMB to blue $MB^+$.

| Reaction | | | $E^0$ (V) | Eq. |
|---|---|---|---|---|
| $Fe^{2+} + 2\ e^-$ | $\Leftrightarrow$ | $Fe^0$ | -0.44 | (1) |
| $Fe^{3+}_{(s)} + e^-$ | $\Leftrightarrow$ | $Fe^{2+}_{(s)}$ | -0.36 to -0.65 | (2) |
| $MB^+ + 2\ e^- + H^+$ | $\Leftrightarrow$ | LMB | 0.01 | (3) |
| $Fe^{3+}_{(aq)} + e^-$ | $\Leftrightarrow$ | $Fe^{2+}_{(aq)}$ | 0.77 | (4) |
| $O_{2(aq)} + 2\ H_2O + 4\ e^-$ | $\Leftrightarrow$ | $4\ OH^-$ | 0.81 | (5) |
| $MnO_2 + 4\ H^+ + 2\ e^-$ | $\Leftrightarrow$ | $Mn^{2+}_{(aq)} + 2\ H_2O$ | 1.23 | (6) |

Reductive MB discoloration in this study may be the result of either (i) $Fe^0$ corrosion (oxidation to $Fe^{II}_{(aq)}$) (Eq. 1) or (ii) oxidation of adsorbed $Fe^{II}$ ($Fe^{II}_{(s)}$ to $Fe^{III}_{(s)}$ - Eq. 2). Additionally, MB adsorption onto in situ generated and aged $Fe^0$ corrosion products and MB entrapment in the structure of forming corrosion products (co-precipitation) are two further discoloration mechanisms. Therefore, it is difficult to resolve the effect of specific redox reactions on MB discoloration from the effects of other processes. To resolve this problem two additives are added to $Fe^0$: granular activated carbon (GAC) and manganese dioxide ($MnO_2$). GAC is a pure adsorbent for MB [25] whereas reductive dissolution of $MnO_2$ has been reported to decolorize

MB [39]. The presentation above shows that $MnO_2$ should re-oxidise reduced LMB (no discoloration). Therefore, MB discoloration in the presence of $MnO_2$ could only result from adsorption. On the other hand, $MnO_2$ is known to be reductively dissolved by $Fe^{II}$ [37, 40]. By consuming $Fe^{II}$, $MnO_2$ accelerates $Fe^0$ corrosion, producing more adsorption or co-precipitation agents for MB. Increased adsorption is supported by the fact that iron corrosion products are of higher specific surface area (> 40 $m^2\ g^{-1}$) than the used $Fe^0$ (0.29 $m^2\ g^{-1}$). The reductive dissolution of $MnO_2$ (Eq. 7 and 8) produce further new reactive adsorbents (MnOOH and FeOOH).

$$Fe^{2+}_{(aq)} + MnO_2 + 2\ H_2O \Rightarrow FeOOH + MnOOH + 2\ H^+ \quad (7)$$

$$2\ Fe^{2+}_{(aq)} + MnO_2 + 2\ H_2O \Rightarrow 2\ FeOOH + Mn^{2+} + 2\ H^+ \quad (8)$$

Noubactep et al. [36] have shown that $MnO_2$ retards the availability of free corrosion products for contaminant co-precipitation.

The used methodology for the investigation of the process of MB discoloration mechanism by $Fe^0$ consists in following the MB discoloration in the presence of $MnO_2$ ("$Fe^0$" and "$Fe^0 + MnO_2$" systems). Thus, the availability of corrosion products for MB co-precipitation in the bulk solution is delayed by the addition of $MnO_2$. It should be kept in mine that MB discoloration and not MB removal is discussed in this study. For the discussion of MB removal TOC measurements for instance should have been necessary to account for MB reduction to LMB which remains in solution.

## Materials and Methods

### Solutions

The MB molecule has a minimum diameter of approximately 0.9 nm [25,41]. As positively charged ions, MB should readily adsorb onto negatively charged surface. That is at $pH > pH_{pzc}$; $pH_{pzc}$ being the pH at the point of zero charge [42,43]. The used initial concentration was 20 mg

135 $L^{-1}$ (~0.063 mM) MB and it was prepared by diluting a 1000 mg $L^{-1}$ stock solution. All chemicals
136 were analytical grade.
137 **Solid Materials**
138 The main $Fe^0$ material (ZVI0 – Tab. 1) is a readily available scrapped iron. Its elemental
139 composition was found to be: C: 3.52%; Si: 2.12%; Mn: 0.93%; Cr: 0.66%. The material was
140 fractionated by sieving. The fraction 1.6 - 2.5 mm was used. The sieved $Fe^0$ was used without
141 any further pre-treatment. Further 13 commercial $Fe^0$ samples (ZVI1 through ZVI13) were used
142 in the set of experiments aiming at characterizing the impact of $Fe^0$ source. The main
143 characteristics of these materials are summarized in table 1, which is quite typical for a large
144 range of powdered and granular $Fe^0$ used in laboratory investigations and field works.
145 The used granular activated carbon (GAC or AC from LS Labor Service GmbH - Griesheim) was
146 crushed and sieved. The particle sized fraction ranging from 0.63 to 1.0 mm was used without
147 further characterization. Granular activated carbon is used as porous adsorbent for MB [25,26].
148 Powdered commercial $Fe_2O_3$ (Fluka), $Fe_3O_4$ (Fisher Scientific) and $MnO_2$ (Sigma-Aldrich) were
149 purchased and used without any further characterization. $Fe_2O_3$ and $Fe_3O_4$ were also used as
150 possible MB adsorbents and are proxies for aged iron corrosion products (Tab. 2).
151 Broken manganese nodules ($MnO_2$) collected from the deep sea with an average particle size of
152 1.5 mm and elemental composition of Mn: 41.8%; Fe: 2.40%; Si: 2.41%; Ni: 0.74%; Zn: 0.22%;
153 Ca: 1.39%; Cu: 0.36% were used. These manganese nodules originated from the pacific ocean
154 (Guatemala- basin: 06°30 N, 92°54 W and 3670 m deep). The target chemically active
155 component is $MnO_2$, which occurs naturally mainly as birnessite and todorokite [44]. $MnO_2$ was
156 mainly used to control the availability of in situ generated oxides from $Fe^0$ corrosion [36, 45].
157 Reductive dissolution of $MnO_2$ has been reported to degrade a number of organic pollutants [39,

158 46 and ref. therein]. Zhu et al. [39] reported the quantitative discoloration of MB by deep sea
159 manganese nodules (pelagite).

160 **Rationale for Choice of Test Conditions**

161 Materials selected for study were known to be effective for adsorbing MB (GAC), discoloring
162 MB ($Fe^0$, $MnO_2$) or delaying the availability of iron corrosion products in $Fe^0/H_2O$ systems
163 ($MnO_2$). $Fe_2O_3$ and $Fe_3O_4$ were used to characterize the reactivity of aged corrosion products.
164 Table 2 summarises the function of the individual materials and gives the material surface
165 coverage in individual reaction vessels. The detailed method for the calculation of the surface
166 coverage ($\theta$) is presented by Jia et al. [47]. The minima of reported specific surface area (SSA)
167 values of the adsorbents were used for the estimation of surface coverage. The $Fe^0$ SSA was
168 earlier measured by Mbudi et al. [52]. The value 120 $Å^2$ is considered for the molecular cross-
169 sectional area of MB [25]. From Tab. 2 it can be seen that, apart from $Fe^0$ ($\theta = 31$), all other
170 materials were present in excess "stoichiometry" ($\theta \leq 0.2$). This means that the available surface
171 of $Fe^0$ can be covered by up to 31 mono-layers of MB, whereas the other materials should be
172 covered only to one fifth with MB ($\theta = 1$ corresponds to a mono-layer coverage). Therefore,
173 depending on the initial pH value and the affinity of MB for the individual materials ($pH_{pzc}$) and
174 the kinetics of MB diffusion to the reactive sites (material porosity, mixing intensity), the MB
175 discoloration should be quantitative. A survey of the $pH_{pzc}$ values given in Tab. 2 suggests that
176 MB adsorption onto all used adsorbents should be favourable because the initial pH was 7.8. At
177 this pH value all surfaces are negatively charged; MB is positively charged. Because the available
178 $Fe^0$ surface can be covered by up to 31 layers of MB, a progressive MB discoloration in presence
179 of $Fe^0$ is expected. The tests were performed under mechanically non-disturbed conditions; the
180 effect of the shaking intensity was evaluated in separated experiments. Because diffusion is the

main mechanism of MB transport under non-disturbed conditions, long reaction times were experienced to identify the main process of aqueous MB discoloration by $Fe^0$.

**Discoloration studies**

Unless otherwise indicated, batch experiments without shaking were conducted. The batches consisted of 5 g $L^{-1}$ of a reactive material (GAC, $Fe^0$, $Fe_2O_3$, $Fe_3O_4$, $MnO_2$). In some experiments 5 g $L^{-1}$ $Fe^0$ was mixed with 0 or 5 g $L^{-1}$ AC and $MnO_2$ respectively. An equilibration time of about 30 days was selected to allow a MB discoloration efficiency of about 80% in the reference system (ZVI0 alone). The extent of MB discoloration by AC, $Fe^0$, $MnO_2$, aged ($Fe_2O_3$, $Fe_3O_4$) and in situ generated iron oxides was characterized. For this purpose 0.11 g of $Fe^0$ and 0 or 0.11 g of the additive were allowed to react in sealed sample tubes containing 22.0 mL of a MB solution (20 mg $L^{-1}$) at laboratory temperature (about 20° C). The tubes (20 mL graded) were filled to the total volume to reduce the head space in the reaction vessels. Initial pH was ~7.8. After equilibration, up to 5 mL of the supernatant solutions were carefully retrieved (no filtration) for MB measurements. In order to fit the calibration curve for quantitative measurements, the maximal dilution factor was four (4).

Apart from experiments aiming at investigating the impact of mixing intensity and that of the initial pH value, the contact vessels were turned over-head at the beginning of the experiment and allowed to equilibrate in darkness to avoid possible photochemical side reactions. At the end of the equilibration time no attempt was made to homogenize the solutions.

**Analytical methods**

MB concentrations were determined by a Cary 50 UV-Vis spectrophotometer at a wavelength of 664.5 nm using cuvettes with 1 cm light path. The pH value was measured by combined glass electrodes (WTW Co., Germany). Electrodes were calibrated with five standards following a multi-point calibration protocol [53] in agreement with the current IUPAC recommendation [54].

Each experiment was performed in triplicate and averaged results are presented.

## Results and Discussion

After the determination of the residual MB concentration (C) the corresponding percent MB discoloration was calculated according to the following equation (Eq. 9):

$$P = [1 - (C/C_0)] * 100\% \quad (9)$$

where $C_0$ is the initial aqueous MB concentration (about 20 mg $L^{-1}$), while C gives the MB concentration after the experiment. The operational initial concentration ($C_0$) for each case was acquired from a triplicate control experiment without additive material (so-called blank). This procedure was to account for experimental errors during dilution of the stock solution (1000 mg $L^{-1}$), MB adsorption onto the walls of the reaction vessels and all other possible side reaction during the experiments.

### MB discoloration by different agents and discoloration mechanism by $Fe^0$

Figure 1 shows the time dependent MB discoloration curve for all the investigated materials. The reference system is a blank experiment as presented above. It can be seen that commercial $Fe_2O_3$ and $MnO_2$ did not significantly decolourise MB over the whole duration of the experiments. It is well-known, that poorly crystalline natural $MnO_2$ are more reactive than land-born and synthetic $MnO_2$ [39,44]. The decreasing order of discoloration efficiency at the end of the experiment was: $Fe^0$ > GAC > $Fe_3O_4$ > $MnO_2$. However, the evolution of the individual systems was very different.

(i) As expected from the surface coverage ($\theta = 31$), $Fe^0$ presents a progressive MB discoloration over the duration of the experiment. The discoloration mechanism can be the reduction to LMB by $Fe^0$ and $Fe^{II}_{(s)}$ species, adsorption onto in situ generated corrosion products and/or MB co-precipitation with these new corrosion products.

228 (ii) $Fe_3O_4$ (20 g $L^{-1}$) shows a rapid discoloration kinetic for the first 8 days. The discoloration
229 efficiency then remains constant to approximately 60% through the end of the experiment. This
230 behaviour is typical for non-porous adsorbents. Alternatively available pores may be inaccessible
231 for MB.
232 (iii) MB discoloration through GAC is insignificant at the start of the experiment (10% after 10
233 days) and then increases progressively to 75% at the end of the experiment (day 36). This
234 behaviour is typical for porous adsorbents.
235 (iv) $MnO_{2\ (nat)}$ shows the same behaviour as GAC but the extent of MB discoloration is
236 significantly lower (50% at day 36). Natural $MnO_2$ acts mostly as adsorbent. MB oxidative
237 discoloration as reported Zhu et al. [39] is not likely to occur under the experimental conditions
238 of this work. Note that, on the contrary to Zhu et al. [39], the experiments in this study were
239 performed under mechanically non-disturbed conditions. While investigating the effect of
240 dynamic conditions, Zhu et al. [39] did not include any non-disturbed system. They just
241 compared shaking (145 $min^{-1}$) *versus* motor-stirring (550 $min^{-1}$) and air-bubbling *versus* nitrogen
242 bubbling (both 32 mL $s^{-1}$). These mixing conditions are pertinent to wastewater treatment
243 systems but are not reproducible in field-$Fe^0$ treatment walls, mixing could have favour MB
244 mineralisation (oxidation to $CO_2$) which is an irreversible discoloration.
245 To better characterize the MB discoloration from aqueous solution by $Fe^0$, five further
246 experiments have been performed for 36 days with 5 g $L^{-1}$ $Fe^0$ and 0 or 5 g $L^{-1}$ of GAC and
247 natural $MnO_2$.
248 Figure 2a summarizes the results of MB discoloration in these five systems and Fig. 2b depicts
249 the evolution of MB discoloration for 5 g $L^{-1}$ $Fe^0$ and additive (AC or $MnO_2$) dosages varying
250 from 0 to 9 g $L^{-1}$ for an experimental duration of 36 days. Fig. 2a shows a regular evolution for
251 the systems involving AC and $Fe^0$. The MB discoloration efficiency decreases in the order "$Fe^0$ +

252 AC" > $Fe^0$ > AC. Considering AC and $Fe^0$ as pure adsorbents it is expected that the mixture
253 (maximal available binding sites) depicts a larger MB discoloration efficiency than individual
254 materials (Tab. 2). This trend was not observed for systems involving $MnO_2$. Here, the
255 decreasing order of MB discoloration efficiency was: $Fe^0$ > "$Fe^0$ + $MnO_2$" ≅ $MnO_2$. These
256 observations were described by Noubactep et al. [36,45,55] for uranium removal by $Fe^0$. A
257 "$MnO_2$ test" was proposed for mechanistic investigations in $Fe^0/H_2O$ systems. The major feature
258 of the "$MnO_2$ test" is that in reacting with $Fe^{II}$ from $Fe^0$ oxidation, $MnO_2$ delays the availability
259 of "free" corrosion products which entrapped contaminants while polymerising and precipitating.
260 "Free" corrosion products are Fe-oxides generated in the vicinity of metallic iron grains. As long
261 as $MnO_2$ is reductively dissolved, Fe-oxides are generated at its surface or in its vicinity.
262 Thereafter, if co-precipitation is the primary mechanism of contaminant removal, no quantitative
263 removal could occur until enough free corrosion products are available to entrap them while
264 ageing [36]. To confirm this statement the experiment presented in Fig. 2b was conducted.
265 From Fig. 2b it can be seen that about 4 g $L^{-1}$ activated carbon are sufficient to achieve almost
266 100% MB discoloration. For [AC] > 4 g $L^{-1}$ no additional discoloration was possible. The system
267 with $MnO_2$ depicts a progressive decrease of MB discoloration with increasing $MnO_2$ mass
268 loading. The reaction of $Fe^{II}$ species yielding reductive dissolution of $MnO_2$ is well documented
269 [37,40,56] and yields more adsorbents (e.g., FeOOH, MnOOH – Eq. 7 and 8). However, MB
270 discoloration is only quantitative when the oxidative capacity of available $MnO_2$ for $Fe^{II}$ is
271 exhausted. Thus, MB is removed from the aqueous solution through co-precipitation with in situ
272 generated iron corrosion products. The characterization of the impact of $MnO_2$ on contaminant
273 removal by $Fe^0$ occurs ideally under non-disturbed conditions [57]. Note that, if the experiments
274 are performed under (too high) mixing conditions or in columns, increased contaminant removal
275 efficiency in the presence of $MnO_2$ could have been reported. For example, Burghardt and

Kassahun [58] reported increased uranium and radium removal in "$Fe^0$ + $MnO_2$" systems comparatively to the system with $Fe^0$ alone. The results of Burghardt and Kassahun [58] are by no means contradictory to those reported here and elsewhere [40] because the net effect of $MnO_2$ is to promote iron hydroxide formation (or to sustain corrosion) resulting in an increased contaminant removal capacity. Similarly, while Noubactep et al. [36,45,57] reported a delay of U removal by $Fe^0$ in the presence of pyrite in non-disturbed experiments, Lipczynska-Kochany et al. [59] reported increased carbon tetrachloride degradation in the presence of pyrite. Pyrite is known for its pH lowering capacity, and thus increasing iron corrosion. Non-disturbed experiments allow a better characterization of the progression of involved processes.

**Effect of $Fe^0$ source**

Experiments were conducted with 14 different $Fe^0$ materials: ZVI0 through ZVI13. ZVI1, ZVI2, ZVI3 and ZVI12 were powdered materials. The 10 other samples were granulated materials. The results of MB discoloration are summarised in table 1. The experimental duration was 35 days. It is shown that powdered materials are more efficient in removing MB than granulated materials (Tab. 1). The discoloration efficiency for granulated materials varies from 65% for ZVI7 to 80% for ZVI2 (absolute values). That is 15% reactivity difference while the maximum standard deviation for the triplicates in individual experiments was 8.5% (for ZVI12). Therefore, the $Fe^0$ source (intrinsic reactivity) is a significant operational parameter for laboratory studies. Similar results were reported by Miehr et al. [60] who reported differences in constants of contaminant reduction up to four orders of magnitude when comparing nine types of $Fe^0$. Therefore, comparing results obtained with different granulated $Fe^0$ under comparable experimental conditions may lead to erroneous conclusions.

**Effect of shaking intensity**

Figure 3 clearly shows that MB discoloration efficiency increases with the shaking intensity. The experimental duration was 24 h (1 day). The reaction vessels were shaken on a rotary shaker. The MB discoloration rate of 5% at 0 $min^{-1}$ (non-disturbed conditions) increased to 96% at 200 $min^{-1}$. Between 100 and 150 $min^{-1}$ the MB discoloration rate was constant to 55%. Parallel experiments in 100 mL Erlenmeyer shows comparative results but at 200 $min^{-1}$ the solution was no more limpid and depicted a brown coloration that persisted even after the solutions were allowed to settle for 5 hours. Therefore, a mixing intensity of about 150 $min^{-1}$ can be seen as the critical intensity below which MB discoloration studies should be performed. Since applied mixing intensities have not been tested in preliminary works, it is likely that some used mixing operations have been too massive and impractical to mimic subsurface conditions [11]. Mixing intensities as higher as 500 $min^{-1}$ [61,62] have been used to "keep the iron powder suspended".

Generally, $Fe^0$-based materials show greater contaminant removal efficiency under mixed than under non-disturbed conditions. This removal efficiency is usually attributed to direct reduction whenever the thermodynamics are favourable. However, the open literature on mixed batch experiments demonstrates that a minimum mixing intensity (bubbling, shaking or stirring) is required for complete suspension of solid particles in a liquid medium (e.g., an aqueous solution). Below this critical mixing intensity, the total surface area of the investigated particles is not directly accessible for reaction and the rate of mass transfer depends strongly on stirring rate. Kinetic studies aiming at distinguishing between diffusion-controlled and chemistry-controlled processes have to be conducted at mixing intensities above this critical value [56]. Noubactep [11] has demonstrated that experiments in $Fe^0/H_2O$ systems aiming at investigating processes pertinent to subsurface situations should be conducted below the critical value (mass transfer dependent). For $Fe^0$, it is obvious, that the value of this critical mixing intensity depends on the

322 particle size (nm, µm, mm). Choe et al. [63] reported a critical value of 40 $min^{-1}$ for nano-scale
323 $Fe^0$ and performed their experiments at a mixing intensity of 60 $min^{-1}$. According to the
324 presentation above, Choe et al. [63] would have worked with mixing intensities below 40 $min^{-1}$ to
325 obtain results relevant for groundwater conditions. Furthermore, working at mixing intensities
326 above 40 $min^{-1}$ accelerates iron corrosion yielding more corrosion products which are equally
327 kept suspended in the reaction medium. In the course of corrosion products formation,
328 contaminants are entrapped in the matrix of iron oxides (co-precipitation). It is well know that
329 even low adsorbable species are readily removed from aqueous solutions when precipitation
330 occurs in their presence [16,17,20,21]. As discussed above, MB discoloration mainly occurs
331 through co-precipitation with newly generated corrosion products (see above: "MB discoloration
332 by different agents and discoloration mechanism by $Fe^0$"). MB discoloration by aged corrosion
333 products was insignificant ($Fe_2O_3$) or very limited ($Fe_3O_4$).

334 **Effect of the initial pH value**

335 The effect of the initial pH on MB discoloration was investigated over the pH range of 1.5 to
336 10.0. The initial pH was adjusted by addition of 1.0 M NaOH or HCl. The experiments were
337 conducted under shaken conditions (100 $min^{-1}$). The pH of the solutions was monitored at the end
338 of the experiments (24 and 48 h). The results are summarised in Fig. 4. MB discoloration was
339 negligible when the final pH was lower than 4 ($P < 10\%$). Once the finial pH exceeded this
340 critical value, MB quantitative discoloration occurred and the extent was pH-independent (60%
341 after 24 h and 76% after 48 h). This observation is consistent with the two main types of aqueous
342 iron corrosion under oxic conditions [64,65]: (i) hydrogen evolution type ($pH < 4$) and (ii) oxygen
343 absorption type ($pH > 4$). The characteristic feature of "hydrogen evolution corrosion" is the
344 liberation of hydrogen as hydrogen gas ($H_2$) at the cathode. Hydrogen evolution corrosion is
345 normally associated with acid electrolytes (e.g., acid mine drainage) and is not relevant for the

346 majority of groundwaters, unless the aquifer is strictly anoxic. The “oxygen absorption” type of
347 immersed $Fe^0$ corrosion is characteristic of neutral waters. At these pH values (pH > 4.0) iron
348 solubility is low [66]. Thus iron oxide precipitates and MB are removed from the aqueous
349 solution by sequestration (co-precipitation). The results from Fig. 4 validate the concept that all
350 contaminants are primarily adsorbed or/and sequestered by iron corrosion products (co-
351 precipitation) [11,12]. In fact MB discoloration was quantitative only at final pH > 4, where iron
352 oxides precipitate due to the low solubility of Fe. Within the oxide-film, redox reactions driven
353 by $Fe^{II}$ species have been reported [67]. Therefore, co-precipitated MB can be reduced to LMB
354 but this reaction could not contribute to recorded MB discoloration.
355 A certain commonly misconception may be found in the literature concerning the process of
356 contaminant removal in $Fe^0/H_2O$ systems due to improper consideration of the two main
357 mechanisms of iron corrosion. Ideally, whenever the initial pH is lower than 4, the pH should be
358 carefully monitored and used to interpret results. From Fig. 4 it can be seen for example, that for
359 an initial pH of 3.0 the final pH was 4.3 and the extent of MB discoloration was slightly lower
360 than that of the experiment with initial pH values $\geq$ 4 (for the given experimental duration).
361 Consequently, the repeatedly reported lag time for contaminant removal [61,68] is the time to
362 exceed pH 4 (or to enable generation of enough corrosion products for contaminant co-
363 precipitation/sequestration). It must be emphasised that for contaminants (e.g., $Cr^{IV}$) which are
364 also reducible by aqueous $Fe^{II}$ the extent of their removal at pH < 4 depends on their relative
365 solubility of their reduced form. Regardless from the redox reactivity co-precipitation of
366 contaminant and reaction products occurs at pH > 4. Contaminants, intermediates and final
367 products are possibly entrapped in the matrix of corrosion products.

**Effect of solution chemistry**

The effect of solution parameters on MB discoloration by $Fe^0$ was studied using 0.2 mM of $Al(NO)_3$, $BaCl_2$, $CaCl_2$, $CuCl_2$, EDTA, $(NH_4)_2CO_3$, and $NiCl_2$. Further non-disturbed experiments were performed for 35 days with concentrations of $CaCl_2$, $CuCl_2$ and $NaHCO_3$ varying from 0 to 4 mM (Figure 5). Figure 5a shows that apart from $(NH_4)_2CO_3$ (90%) all other additives lower the extent of MB discoloration by $Fe^0$ (78%). The lowest discoloration efficiency (15%) was observed in the presence of EDTA and is consistent with the fact that complexing $Fe^{II}/Fe^{III}$ delays the iron oxide precipitation [69-71] and hence retards MB discoloration. For the four systems containing chloride ions ($Cl^-$), $NiCl_2$ depicts the lowest MB discoloration efficiency (33%) and $CaCl_2$ the highest (72%). $BaCl_2$ and $CuCl_2$ show very comparable discoloration efficiency (about 60%). This observation is partly consistent with reported results from the literature on corrosion stating that: (i) at low concentration $CO_2^{3-}$ is corrosive, (ii) hardness ($Ca^{2+}$) is corrosive, while $Ni^{2+}$ has inhibitive properties for iron corrosion. $Cu^{2+}$ would have accelerated $Fe^0$ corrosion yielding more corrosion products for MB discoloration than in the reference system ($Fe^0$ alone). Because this was not the case, the experiments reported in Fig. 5b were performed.

It can be seen that $NaHCO_3$ enhances MB discoloration for all tested concentrations. The discoloration efficiency increased from 77% at 0.0 mM $NaHCO_3$ to 90% at 0.8 mM $NaHCO_3$ and remains constant for higher $NaHCO_3$ concentrations ($\leq$ 4 mM). In the experiments with $CaCl_2$ and $CuCl_2$ the initial discoloration rate of 77% first decreases to 70 and 64% respectively at an additive concentration of 0.2 mM and subsequently increases to about 74% and remains constant. However, for 4 mM $CuCl_2$ the discoloration efficiency (73% at 2 mM) drops to 30% at 4 mM while the discoloration efficiency in the presence of $CaCl_2$ remains constant (74%). The behaviour of the system with $CuCl_2$ was not further investigated but suggests that if $Cu^{2+}$ is quantitatively produced in a Cu/Fe bimetallic system the reactivity of $Fe^0$ may be inhibited. This

392 issue is yet to be considered in the $Fe^0$ technology. Similarly, the comparatively low discoloration
393 efficiency observed in the system with 0.2 mM $NiCl_2$ (33% against 60% for $CaCl_2$) should
394 question the concept of using Ni and Cu as additive metals to form nickel bimetallic systems to
395 "improve the reduction capacity of $Fe^0$" [28]. No such improvement could be observed in this
396 study (Fig. 5). Discussing the validity of the concept of using bimetallics to improve $Fe^0$
397 reactivity is over the scope of this work (see ref. [72]).
398 Another important issue from the discussion above is the importance of the cation nature in
399 chloride salts on the extent of MB removal. Generally, chloride ions are known to promote iron
400 corrosion, and therefore increase, sustain or restore $Fe^0$ reactivity. These observations are mostly
401 attributed to pitting iron corrosion or avoiding the formation of oxide-layers on iron [73, 74]. The
402 discussion above demonstrated clearly that the nature of the used salt should be considered in
403 comparing results from independent sources.

404 **Conclusions**

405 In summary, despite the low adsorptivity exhibited by MB towards $Fe^0$, $Fe_2O_3$ and $Fe_3O_4$, under
406 the experimental conditions, MB was quantitatively discolored as $Fe^0$ corrosion proceeded. The
407 extent of MB discoloration was insignificant in experiments in which the availability of in situ
408 generated corrosion products was delayed ($MnO_2$ addition). Data from the experiments with the
409 systems "$Fe^0$" and "$MnO_2$" clearly showed that the kinetics of MB adsorption and reduction by
410 $MnO_2$ is slower than MB co-precipitation. Thus, even in systems where direct contaminant
411 reduction (electrons from $Fe^0$) is likely to occur, co-precipitation will interfere with (or even
412 hamper) mass transport involving $Fe^0$.
413 The concept that methylene blue (MB) discoloration from aqueous solution in presence of
414 metallic iron is caused by MB co-precipitation with $Fe^0$ corrosion products is consistent with
415 many experimental observations, in particular the effects of the initial pH value and the impact of

416 $MnO_2$ on MB discoloration. Generally, aqueous contaminant removal in $Fe^0/H_2O$ systems can be
417 viewed as a “trickle down” in which a fraction of the targeted contaminant is continuously adsorb
418 onto in situ generated high reactive corrosion products [11]. Contaminants are subsequently
419 entrapped into the structure of ageing corrosion products. In this situation, no observable
420 equilibrium is attained. Therefore, the use of adsorption isotherms (e.g., Freundlich, Langmuir) to
421 interpret data from removal experiments in $Fe^0/H_2O$ systems is not justified (e.g. ref. [75]).
422 Furthermore, adsorbed or co-precipitated contaminants can be further reduced both by a direct
423 and an indirect mechanism [11.12]. The direct contaminant reduction is only possible when the
424 oxide-film on $Fe^0$ is electronic conductive or if so-called electron mediators are available [34,
425 76]. Noubactep [11] has clearly shown that the concept of contaminant adsorption and co-
426 precipitation as fundamental removal mechanism is more accurate and considers inherent
427 mistakes of the reductive transformation concept.
428 It must be concluded that natural $Fe^0/H_2O$ systems consist of core $Fe^0$ and essentially amorphous
429 Fe oxides that remain to be characterized. In this regard, many investigators have shown the
430 presence of various Fe oxyhydroxides and discussed their role in the process of contaminant
431 removal [77-82]. Strictly, these oxyhydroxides should be considered as transient states as
432 $Fe^0/H_2O$ systems are transforming systems. Therefore, a continuously reacting $Fe^0/H_2O$ system
433 can not be simply treated being at thermodynamic equilibrium. Thus, characterising the system
434 composition at certain dates is very useful but should be completed by continuously
435 characterizing the system as the contaminants are removed and/or transformed.
436 With this study, the potential of bulk reactions with selected additives for providing mechanistic
437 information [36] on aqueous contaminant removal is confirmed for the first time using an organic
438 compound. This study also demonstrates the significant impact of selected operational
439 experimental parameters (iron type, shaking intensity, solution chemistry) on the process of MB

co-precipitation in $Fe^0/H_2O$ systems. A unified experimental procedure is needed to: (i) avoid further data generation under non relevant experimental conditions, and (ii) facilitate the inter-laboratory comparison of data. At the term such efforts will provide a confident background for a non-site-specific iron barrier design [83]. Keeping in mine the large spectrum of contaminants that can be removed in $Fe^0/H_2O$ systems and the diversity of $Fe^0$ materials that are used by individual research groups, it is obvious, that the development of such an unified experimental procedure should be a concerted effort.

**Acknowledgments**

For providing the iron materials ($Fe^0$) investigated in this study the author would like to express his gratitude to the branch of the MAZ (Metallaufbereitung Zwickau, Co) in Freiberg (Germany), Gotthart Maier Metallpulver GmbH (Rheinfelden, Germany), Connelly GPM Inc. (USA), Dr. R. Köber from the Institute Earth Science of the University of Kiel and Dr.-Ing. V. Biermann from the Federal Institute for Materials Research and Testing (Berlin, Germany). Mechthild Rittmeier and Emin Özden are acknowledged for technical support. The work was granted by the Deutsche Forschungsgemeinschaft (DFG-No 626/2-2).

**References**

[1] A.D. Henderson, A.H. Demond, Long-term performance of zero-valent iron permeable reactive barriers: a critical review. Environ. Eng. Sci. 24 (2007), 401–423.

[2] D.F. Laine, I.F. Cheng, The destruction of organic pollutants under mild reaction conditions: A review. Microchem. J. 85 (2007), 183–193.

[3] S.F. O´Hannesin, R.W. Gillham, Long-term performance of an in situ "iron wall" for remediation of VOCs. Ground Water 36 (1998), 164–170.

463 [4] M.M. Scherer, S. Richter, R.L. Valentine, P.J.J. Alvarez, Chemistry and microbiology of
464 permeable reactive barriers for in situ groundwater clean up. Rev. Environ. Sci. Technol. 30
465 (2000), 363–411.
466 [5] P.G. Tratnyek, M.M. Scherer, T.J. Johnson, L.J. Matheson, Permeable reactive barriers of
467 iron and other zero-valent metals. In Chemical Degradation Methods for Wastes and
468 Pollutants: Environmental and Industrial Applications, Tarr, M.A., Ed., Marcel Dekker: New
469 York, (2003) 371–421.
470 [6] N.A. VanStone, R.M. Focht, S.A. Mabury, B.S. Lollar, Effect of iron type on kinetics and
471 carbon isotopic enrichment of chlorinated ethylenes during abiotic reduction on Fe(0).
472 Ground Water 42 (2004), 268–276.
473 [7] S.D. Warner, D. Sorel, Ten years of permeable reactive barriers: Lessons learned and future
474 expectations. In: Chlorinated Solvent and DNAPL Remediation: Innovative Strategies for
475 Subsurface Cleanup, Henry, S.M., Warner, S.D., Eds, American Chemical Society:
476 Washington, DC, ACS Symp., Ser. 837 (2003), 36–50.
477 [8] Y. You, J. Han, P.C. Chiu, Y. Jin, Removal and inactivation of waterborne viruses using
478 zerovalent iron. Environ. Sci. Technol. 39 (2005), 9263–9269.
479 [9] B. Jafarpour, P.T. Imhoff, P.C. Chiu, Quantification and modelling of 2,4-dinitrotoluene
480 reduction with high-purity and cast iron. J. Contam. Hydrol. 76 (2005), 87–107.
481 [10] J.A. Mielczarski, G.M. Atenas, E. Mielczarski, Role of iron surface oxidation layers in
482 decomposition of azo-dye water pollutants in weak acidic solutions. Appl. Catal. B56 (2005),
483 289–303.
484 [11] C. Noubactep, Processes of contaminant removal in "$Fe^0$–$H_2O$" systems revisited. The
485 importance of co-precipitation. Open Environ. J. 1 (2007), 9–13.

[12] C. Noubactep, A critical review on the mechanism of contaminant removal in $Fe^0$–$H_2O$ systems. Environ. Technol. 29 (2008), 909–920.

[13] M. Cohen, The formation and properties of passive films on iron. Can. J. Chem. 37 (1959), 286–291.

[14] K.J. Vetter, General kinetics of passive layers on metals. Electrochim. Acta 16 (1971), 1923–1937.

[15] B. Gu, J. Schmitt, Z. Chen, L. Liang, J.F. McCarthy, Adsorption and desorption of natural organic matter on iron oxide: mechanisms, and models. Environ. Sci. Technol. 28 (1994), 38–46.

[16] Y. Satoh, K. Kikuchi, S. Kinoshita, H. Sasaki, Potential capacity of coprecipitation of dissolved organic carbon (DOC) with iron(III) precipitates. Limnology 7 (2006), 231–235.

[17] U. Schwertmann, F. Wagner, H. Knicker, Ferrihydrite–Humic associations magnetic hyperfine interactions. Soil Sci. Soc. Am. J. 69 (2005), 1009–1015.

[18] W.-C. Ying, J.J. Duffy, M.E. Tucker, Removal of humic acid and toxic organic compounds by iron precipitation. Environ. Progr. 7 (1988), 262–269.

[19] E. Tipping, The adsorption of aquatic humic substances by iron oxides. Geochim. Cosmochim. Acta 45 (1981), 191–199.

[20] E. Tipping, Some aspects of the interactions between particulate oxides and aquatic humic substances. Mar. Chem. 18 (1986), 161–169.

[21] R.J. Crawford, I.H. Harding, D.E. Mainwaring, Adsorption and coprecipitation of single heavy metal ions onto the hydrated oxides of iron and chromium. Langmuir 9 (1993), 3050–3056.

[22] H. Füredi-Milhofer, Spontaneous precipitation from electrolytic solutions. Pure Appl. Chem. 53 (1981), 2041–2055.

510 [23] I. Nirdosh, S.V. Muthuswami, M.H.I. Baird Radium in uranium mill tailings - Some
511 observations on retention and removal. Hydrometallurgy 12 (1984), 151–176.
512 [24] B.D. Jones, J.D. Ingle, Evaluation of redox indicators for determining sulfate-reducing and
513 dechlorinating conditions. Water Res. 39 (2005), 4343–4354.
514 [25] A.A. Attia, B.S. Girgis, N.A. Fathy, Removal of methylene blue by carbons derived from
515 peach stones by $H_3PO_4$ activation: Batch and column studies. Dyes and Pigments 76 (2008),
516 282–289.
517 [26] J. Avom, J.B. Ketcha, C. Noubactep, P. Germain, Adsorption of methylene blue from an
518 aqueous solution onto activated carbons from palm-tree cobs. Carbon 35 (1997), 365–369.
519 [27] Dutta, K., Mukhopadhyay, S., Bhattacharjee, S., Chaudhuri, B., 2001. Chemical oxidation of
520 methylene blue using a Fenton-like reaction. J. Hazard. Mater. 84, 57–71.
521 [28] L.M. Ma, Z.G. Ding, T.Y. Gao, R.F. Zhou, W.Y. Xu, J. Liu, Discoloration of methylene
522 blue and wastewater from a plant by a Fe/Cu bimetallic system. Chemosphere 55 (2004),
523 1207–1212.
524 [29] S. Pande, S.K. Ghosh, S. Nath, S. Praharaj, S. Jana, S. Panigrahi, S. Basu, T., Pal, Reduction
525 of methylene blue by thiocyanate: Kinetic and thermodynamic aspects. J. Colloid Interf.
526 Sci. 299 (2006), 421–427.
527 [30] K. Imamura, E. Ikeda, T. Nagayasu, T. Sakiyama, K. Nakanishi, Adsorption behavior of
528 methylene blue and its congeners on a stainless steel surface. J. Colloid Interf. Sci. 245
529 (2002), 50–57.
530 [31] E.E. Oguzie, Corrosion inhibition of mild steel in hydrochloric acid solution by methylene
531 blue dye. Mater. Lett. 59 (2005), 1076–1079.
532 [32] J. Cao, L. Wei, Q. Huang, L. Wang, S. Han, Reducing degradation of azo dye by zero-valent
533 iron in aqueous solution. Chemosphere 38 (1999), 565–571.

534 [33] S. Nam, P.G. Tratnyek, Reduction of azo dyes with zero-valent iron. Wat. Res. 34 (2000),
535 1837–1845.
536 [34] E.J. Weber, Iron-mediated reductive transformations: Investigation of reaction mechanism.
537 Environ. Sci. Technol. 30 (1996), 716–719.
538 [35] F. dos Santos Coelho, J.D. Ardisson, F.C.C. Moura, R.M. Lago, E. Murad, J.D. Fabris,
539 Potential application of highly reactive Fe(0)/$Fe_3O_4$ composites for the reduction of Cr(VI)
540 environmental contaminants. Chemosphere 71 (2008), 90–96.
541 [36] C. Noubactep, G. Meinrath, J.B. Merkel, Investigating the mechanism of uranium removal
542 by zerovalent iron materials. Environ. Chem. 2 (2005), 235–242.
543 [37] D. Postma, C.A.J. Appelo, Reduction of Mn-oxides by ferrous iron in a flow system: column
544 experiment and reactive transport modelling. Geochim. Cosmochim. Acta 64 (2000), 1237–
545 1247.
546 [38] A.F. White, M.L. Paterson, Reduction of aqueous transition metal species on the surface of
547 Fe(II)-containing oxides. Geochim. Cosmochim. Acta 60 (1996), 3799–3814.
548 [39] M.-X. Zhu, Z. Wang, L.-Y. Zhou, Oxidative decolorization of methylene blue using
549 pelagite. J. Hazard. Mater. 150 (2008), 37–45.
550 [40] D.F.A. Koch, Kinetics of the reaction between manganese dioxide and ferrous ion. Aust. J.
551 Chem 10 (1957), 150–159.
552 [41] H. Valdes, M. Sanchez-Polo, J. Rivera-Utrilla, C.a. Zaror, Effect of ozone treatment on
553 surface properties of activated carbon. Langmuir 18 (2002), 2111–2116.
554 [42] V. Ender, Zur Struktur der Phasengrenze Metalloxid/Elektrolyt-Potentialbildung und
555 Ladungsbilanz. Acta Hydrochim. Hydrobiol. 19 (1991), 199–208.
556 [43] M.R. Hoffmann, S.T. Martin, W. Choi, D.W. Bahnemann, Environmental applications of
557 semiconductor photocatalysis. Chem. Rev. 95 (1995), 69–96.

[44] J.E. Post, Manganese oxide minerals: Crystal structures and economic and environmental significance. Proc. Natl. Acad. Sci. USA 96 (1999), 3447–3454.

[45] C. Noubactep, A. Schöner, G. Meinrath, Mechanism of uranium (VI) fixation by elemental iron. J. Hazard. Mater. 132 (2006), 202–212.

[46] H. Zhang, C.-H. Huang, Oxidative transformation of triclosan and chlorophene by manganese oxides. Environ. Sci. Technol. 37 (2003), 2421–2430.

[47] Y. Jia, P. Aagaard, G.D. Breedveld, Sorption of triazoles to soil and iron minerals. Chemosphere 67 (2007), 250–258.

[48] T. Liu, D.C.W. Tsang, I.M.C. Lo, Chromium(VI) reduction kinetics by zero-valent iron in moderately hard water with humic acid: iron dissolution and humic acid adsorption. Environ. Sci. Technol. 42 (2008), 2092–2098.

[49] K. Hanna, Adsorption of aromatic carboxylate compounds on the surface of synthesized iron oxide-coated sands. Appl. Geochem. 22 (2007), 2045–2053.

[50] S. Yean, L. Cong., C.T. Yavuz, J.T. Mayo, W.W. Yu, A.T. Kan, V.L. Colvin, M.B. Tomson, Effect of magnetite particle size on adsorption and desorption of arsenite and arsenate. J. Mater. Res. 20 (2005), 3255–3264.

[51] M.I. Bautista-Toledo, J.D. Méndez-Díaz, M. Sánchez-Polo, J. Rivera-Utrilla, M.A. Ferro-García, Adsorption of sodium dodecylbenzenesulfonate on activated carbons: Effects of solution chemistry and presence of bacteria. J. Colloid Interf. Sci. 317 (2008), 11–17.

[52] C. Mbudi, P. Behra, B. Merkel, The Effect of Background Electrolyte Chemistry on Uranium Fixation on Scrap Metallic Iron in the Presence of Arsenic. Paper presented at the Inter. Conf. Water Pollut. Natural Porous Media (WAPO2), Barcelona (Spain) April 11 – 13 (2007), 8 pages.

581 [53] G. Meinrath, P. Spitzer, Uncertainties in determination of pH. Mikrochem. Acta 135 (2000),
582 155–168.
583 [54] R.P. Buck, S. Rondinini, A.K. Covington, F.G.K. Baucke, C.M.A. Brett, M.F. Camoes,
584 M.J.T. Milton, T. Mussini, R. Naumann, K.W. Pratt, P. Spitzer, G.S. Wilson, Measurement of
585 pH. Definition, standards, and procedures (IUPAC Recommendations 2002), Pure Appl.
586 Chem. 74 (2002), 2169–2200.
587 [55] C. Noubactep, G. Meinrath, P. Dietrich, B. Merkel, Mitigating uranium in ground water:
588 prospects and limitations. Environ. Sci. Technol. 37 (2003), 4304–4308.
589 [56] T. Tekin, M. Bayramoglu, Kinetics of the reduction of $MnO_2$ with $Fe^{2+}$ ions in acidic
590 solutions. Hydrometallurgy 32 (1993), 9–20.
591 [57] C. Noubactep, Investigations for the passive in-situ Immobilization of Uranium (VI) from
592 Water (in German). Dissertation, TU Bergakademie Freiberg, Wiss. Mitt. Institut für
593 Geologie der TU Bergakademie Freiberg, Band 21 (2003), 140 pp, ISSN1433-1284.
594 [58] D. Burghardt, A. Kassahun, Development of a reactive zone technology for simultaneous in
595 situ immobilisation of radium and uranium. Environ. Geol. 49 (2005), 314–320.
596 [59] E. Lipczynska-Kochany, S. Harms, R. Milburn, G. Sprah, N. Nadarajah, Degradation of
597 carbon tetrachloride in the presence of iron and sulphur containing compounds. Chemosphere
598 29 (1994), 1477–1489.
599 [60] R. Miehr P.G. Tratnyek, Z.J. Bandstra, M.M. Scherer, J.M. Alowitz, J.E. Bylaska, Diversity
600 of contaminant reduction reactions by zerovalent iron: Role of the reductate. Environ. Sci.
601 Technol. 38 (2004), 139–147.
602 [61] Z. Hao, X. Xu, D. Wang, Reductive denitrification of nitrate by scrap iron filings. J.
603 Zhejiang Univ. Sci. 6B (2005), 182–187.

604 [62] W.S. Pereira, R.S. Freire, Azo dye degradation by recycled waste zero-valent iron powder. J.
605 Braz. Chem. Soc. 17 (2006), 832–838.
606 [63] S. Choe, Y.Y. Chang, K.Y. Hwang, J. Khim, Kinetics of reductive denitrification by
607 nanoscale zero-valent iron, Chemosphere 41 (2000), 1307–1311.
608 [64] G.W. Whitman, R.P. Russel, V.J. Altieri, Effect of hydrogen-ion concentration on the
609 submerged corrosion of steel. Indust. Eng. Chem. 16 (1924), 665–670.
610 [65] E.R. Wilson, The Mechanism of the corrosion of iron and steel in natural waters and the
611 calculation of specific rates of corrosion. Indust. Eng. Chem. 15 (1923), 127–133.
612 [66] D. Rickard, The solubility of FeS. Geochim. Cosmochim. Acta 70 (2006), 5779–5789.
613 [67] M. Stratmann, J. Müller, The mechanism of the oxygen reduction on rust-covered metal
614 substrates. Corros. Sci. 36 (1994), 327–359.
615 [68] C.G. Schreier, M. Reinhard, Transformation of chlorinated organic compounds by iron and
616 manganese powders in buffered water and in landfill leachate. Chemosphere 29 (1994),
617 1743–1753.
618 [69] L.J. Matheson, P.G. Tratnyek, Reductive dehalogenation of chlorinated methanes by iron
619 metal. Environ. Sci. Technol. 28 (1994), 2045–2053.
620 [70] C. Noubactep, G. Meinrath, P. Dietrich, M. Sauter, B. Merkel, Testing the suitability of
621 zerovalent iron materials for reactive walls. Environ. Chem. 2 (2005), 71–76.
622 [71] E.M. Pierce, D.M. Wellman, A.M. Lodge, E.A. Rodriguez, Experimental determination of
623 the dissolution kinetics of zero-valent iron in the presence of organic complexants. Environ.
624 Chem. 4 (2007), 260–270.
625 [72] C. Noubactep, On the operating mode of bimetallic systems for environmental remediation.
626 J. Hazard. Mater. (2008), In Press, Available online 13 August 2008.

627 [73] R. Hernandez, M. Zappi, C.-H. Kuo, Chloride effect on TNT degradation by zerovalent iron
628 or zinc during water treatment. Environ. Sci. Technol. 38 (2004), 5157–5163.
629 [74] J.S. Kim, P.J. Shea, J.E. Yang, J.-E. Kim, Halide salts accelerate degradation of high
630 explosives by zerovalent iron. Environ. Pollut. 147 (2007), 634–641.
631 [75] D.R. Burris, T.J. Campbell, V.S. Manoranjan, Sorption of trichloroethylene and
632 tetrachloroethylene in a batch reactive metallic iron-water system. Environ. Sci. Technol. 29
633 (1995), 2850–2855.
634 [76] P.G. Tratnyek, M.M. Scherer, B. Deng, S. Hu, Effects of natural organic matter,
635 anthropogenic surfactants, and model quinones on the reduction of contaminants by zero-
636 valent iron. Wat. Res. 35 (2001), 4435–4443.
637 [77] P.D. Mackenzie, D.P. Horney, T.M. Sivavec, Mineral precipitation and porosity losses in
638 granular iron columns. J. Hazard. Mater. 68 (1999), 1–17.
639 [78] J.A. Mielczarski, G.M. Atenas, E. Mielczarski, Role of iron surface oxidation layers in
640 decomposition of azo-dye water pollutants in weak acidic solutions. Applied Catalysis B:
641 Environ. 56 (2005), 289–303.
642 [79] D.H. Phillips, B. Gu, D.B. Watson, Y. Roh, L. Liang, S.Y. Lee, Performance evaluation of a
643 zerovalent iron reactive barrier: Mineralogical characteristics. Environ. Sci. Technol. 34
644 (2000), 4169–4176.
645 [80] K. Ritter, M.S. Odziemkowski, R.W. Gillham, An in situ study of the role of surface films
646 on granular iron in the permeable iron wall technology. J. Contam. Hydrol. 55 (2002), 87–
647 111.
648 [81] M.M. Scherer, B.A. Balko, P.G. Tratnyek, The role of oxides in reduction reactions at the
649 metal-water interface. *In* Kinetics and Mechanism of Reactions at the Mineral/Water
650 Interface, Sparks, D.; Grundl, T., Eds; (1999) pp. 301–322.

[82] M.M. Scherer, K. Johnson, J.C Westall, P.G. Tratnyek, Mass transport effects on the kinetics of nitrobenzene reduction by iron metal. Environ. Sci. Technol. 35 (2001), 2804–2811.

[83] K.L. McGeough, R.M. Kalin, P. Myles, Carbon disulfide removal by zero valent iron. Environ. Sci. Technol. 41 (2007), 4607–4612.

**Table 1**: Main characteristics, iron content and percent methylene blue (MB) discoloration (P) of tested $Fe^0$ materials. MB removal were conducted in triplicates for 36 days under non-disturbed conditions. The material code ("code") are from the author, the given form is as supplied; d (µm) is the diameter of the supplied material and the Fe content is given in % mass.

| **Supplier**[a] | **Supplier denotation** | **code** | **form** | **d** (µm) | **Fe** (%) | **P (%)** |
|---|---|---|---|---|---|---|
| **MAZ, mbH** | Sorte 69[b] | ZVI0 | fillings | - | 93[c] | $75 \pm 2$ |
| **G. Maier GmbH** | FG 0000/0080 | ZVI1 | powder | $\leq 80$ | 92[d] | $88 \pm 2$ |
| **G. Maier GmbH** | FG 0000/0200 | ZVI2 | powder | $\leq 200$ | 92[d] | $89 \pm 1$ |
| **G. Maier GmbH** | FG 0000/0500 | ZVI3 | powder | $\leq 500$ | 92[d] | $88 \pm 1$ |
| **G. Maier GmbH** | FG 0300/2000 | ZVI4 | fillings | 200-2000 | 92[d] | $81 \pm 4$ |
| **G. Maier GmbH** | FG 1000/3000 | ZVI5 | fillings | 1000-3000 | 92[d] | $77 \pm 4$ |
| **G. Maier GmbH** | FG 0350/1200 | ZVI6 | fillings | 100-2000 | 92[d] | $88 \pm 1$ |
| **Würth** | Hartgussstrahlmittel | ZVI7 | spherical | 1200 | n.d.[e] | $66 \pm 1$ |
| **Hermens** | Hartgussgranulat | ZVI8 | flat | 1500 | n.d. | $67 \pm 2$ |
| **G. Maier GmbH** | Graugussgranulat | ZVI9 | chips | | n.d. | $71 \pm 7$ |
| **ISPAT GmbH** | Schwammeisen | ZVI10 | spherical | 9000 | n.d. | $72 \pm 6$ |
| **ConnellyGPM** | CC-1004 | ZVI11 | fillings | | >96 | $76 \pm 4$ |
| **ConnellyGPM** | CC-1190 | ZVI12 | fillings | | >96 | $75 \pm 9$ |
| **ConnellyGPM** | CC-1200 | ZVI13 | powder | | >96 | $84 \pm 1$ |

662 [(a)] List of suppliers: MAZ (Metallaufbereitung Zwickau, Co) in Freiberg (Germany); Gotthart Maier

663 Metallpulver GmbH (Rheinfelden, Germany), ISPAT GmbH, Hamburg (Germany), Connelly GPM Inc. (USA),

664 [(b)]Scrapped iron material; [(c)] Mbudi et al. [52]; [(d)] average values from material supplier, [(e)]not determined.

665

665

666 **Table 2**: Characteristics, surface coverage and function of the individual reactive materials of this
667 study. Apart from $Fe^0$ the given value of specific surface area (SSA) for are the minima
668 of reported data. Apart from $Fe_2O_3$ the pH at the point of zero charge ($pH_{pzc}$) is lower
669 than the initial pH value. Therefore, MB adsorption onto the negatively charged
670 surfaces is favorable. The surface coverage is estimated using the method presented by
671 Jia et al. [47]. The total surface that can be covered by the amount of MB present in 22
672 mL of a 0.063 mM is $S_{MB} = 0.997$ $m^2$.

673

| **System** | **$pH_{pzc}$** | **SSA** ($m^2$ $g^{-1}$) | **$S_{available}$** ($m^2$) | **Coverage** (1) | **Function** |
|---|---|---|---|---|---|
| $Fe^0$ | 7.6[a] | 0.29 | 0.032 | 31.3 | MB reductant? |
| $Fe^0 + MnO_2$ | - | - | 4.432 | 0.2 | - |
| $MnO_2$ | 2.0 - 6.0[b] | 40 | 4.4 | 0.2 | delays CP availability |
| $Fe_2O_3$ | 7.5 - 8.8[c] | 60 | 6.6 | 0.2 | mimics aged CP |
| $Fe_3O_4$ | 6.8[d] | 40 | 4.4 | 0.2 | mimics aged CP |
| GAC | 7.0 - 8.0[e] | 200 | 22 | 0.1 | MB adsorbent |
| $Fe^0$ + GAC | - | (-) | 22.032 | 0.1 | - |

674 [a]ref. [48], [b]ref [39], [c]ref. [49], [d]ref. [50], [e]ref. [51].
675

676

677

677 **Figure 1**

678

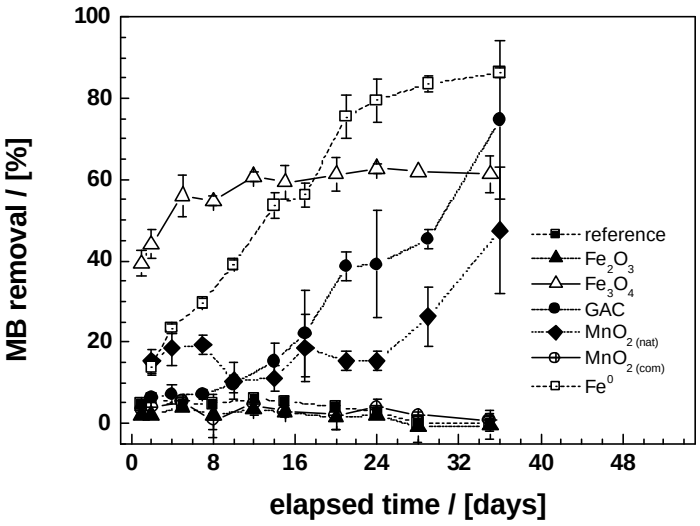


679

680

680 **Figure 2**

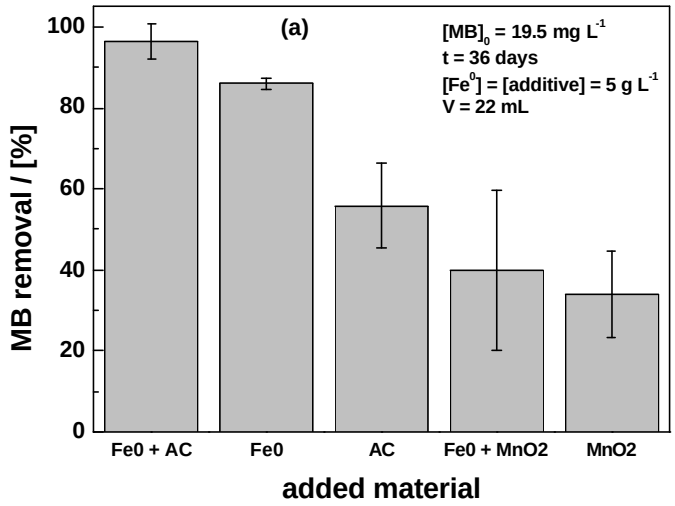


681

682

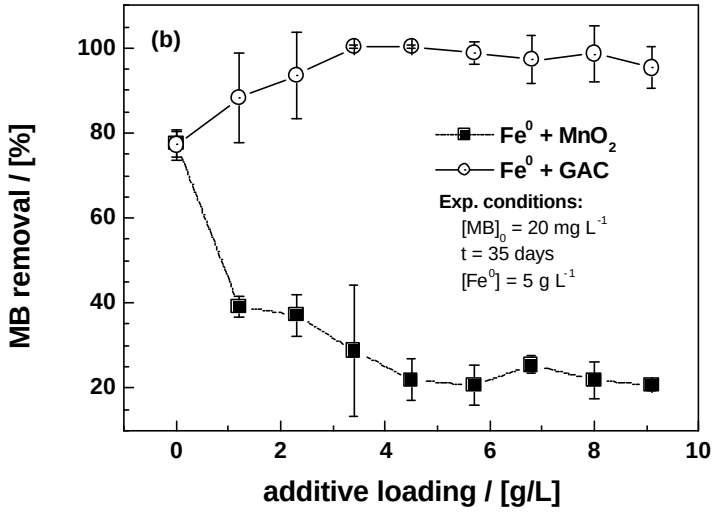


683

684

685

685 **Figure 3**

686

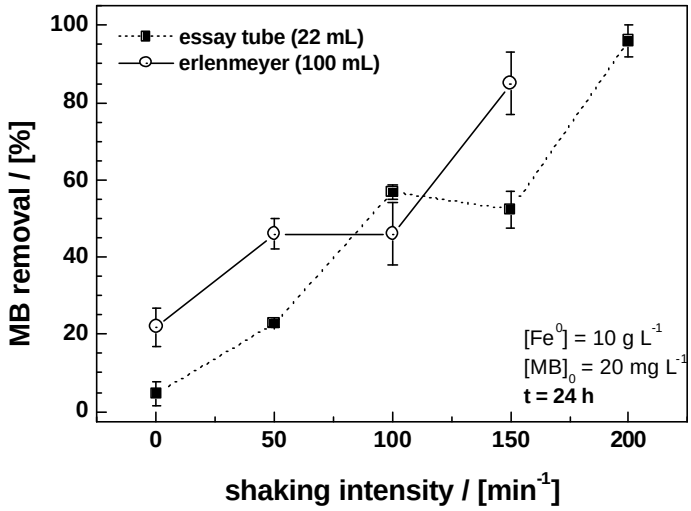


687

688

689

690

690 **Figure 4**

691

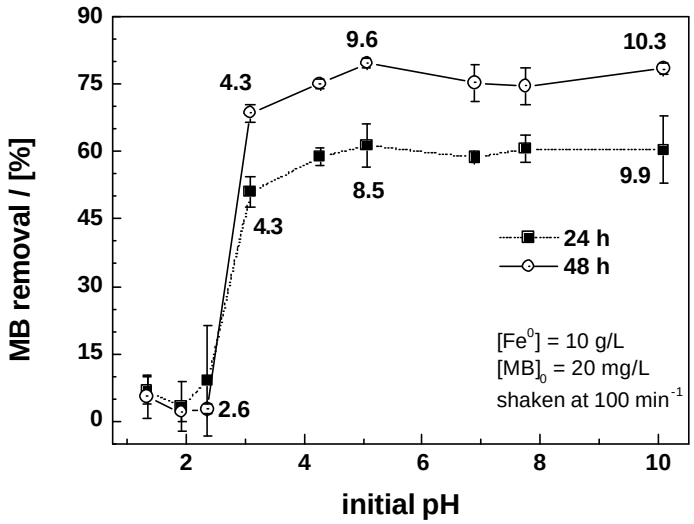


692

693

693 **Figure 5**

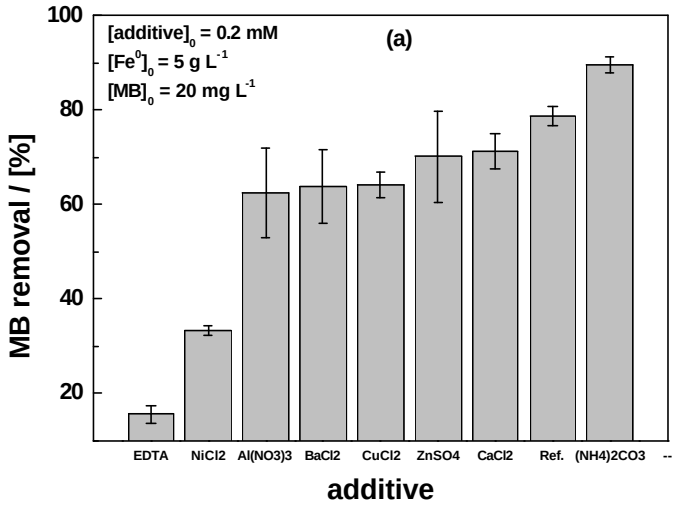


694

695

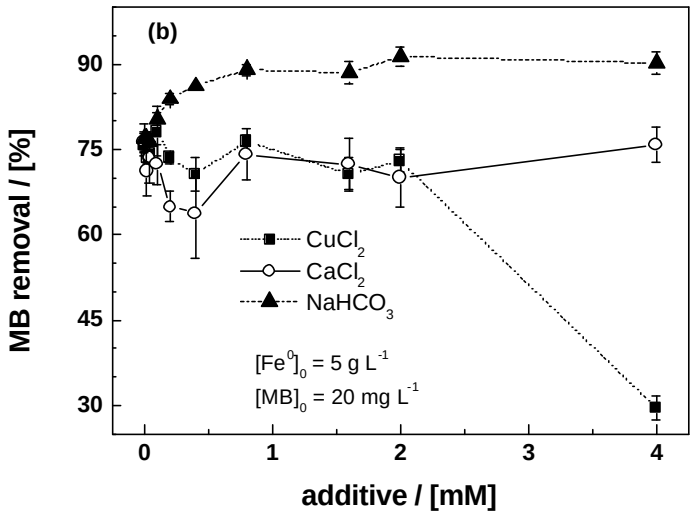


696

697

## Figure Captions

**Figure 1**:

Methylene blue removal (%) as a function of equilibration time for the six tested reactive materials. The reference system is a blank experiment without additives. Two sets of experiments with $MnO_2$ were conducted (see the text). The experiments were conducted in triplicate. Error bars give standard deviations. The lines are not fitting functions, they simply connect points to facilitate visualization.

**Figure 2**:

Methylene blue (MB) discoloration by metallic iron ($Fe^0$), granular activated carbon (AC), manganese nodule ($MnO_2$), and the mixtures "$Fe^0$ + AC" and "$Fe^0$ + $MnO_2$". (a) extent of MB discoloration after 36 days, and (b) dependence of the MB discoloration on the additive loading for 35 days. The experiments were conducted in triplicate. Error bars give standard deviations. The lines are given to facilitate visualization.

**Figure 3**:

Effect of the mixing intensity ($min^{-1}$) on discoloration of MB at initial pH 7.8. The system is mixed on a rotary shaker. The experiments were conducted in triplicate. Error bars give standard deviations. The lines simply connect points to facilitate visualization.

**Figure 4**:

Effect of initial pH on discoloration of MB by $Fe^0$ for 24 and 48 h respectively. The experiments were conducted in triplicate. The reported numbers on the plots are the corresponding final pH values. Error bars give standard deviations. The lines simply connect points to facilitate visualization.

**Figure 5**:

720 Effect of solution chemistry on MB discoloration by metallic iron ($Fe^0$): (a) extent of MB
721 discoloration after 36 days for all tested additives, and (b) dependence of the MB discoloration on
722 selected additive concentrations for 35 days. Ref. in figure “a” refers to the experiment in tap
723 water (“no additive”). The experiments were conducted in triplicate. Error bars give standard
724 deviations. The lines simply connect points to facilitate visualization.